Appendix

Identifying silent COVID-19 infections among children is critical for controlling the pandemic

Seyed M. Moghadas[1], Meagan C. Fitzpatrick[2], Affan Shoukat[3], Kevin Zhang[1,4], and Alison P. Galvani[5]

[1]**Agent-Based Modelling Laboratory, York University, Toronto, Ontario, M3J 1P3 Canada**
[2]**Center for Vaccine Development and Global Health, University of Maryland School of Medicine, 685 W Baltimore St, Baltimore, MD 21201**
[3]**Center for Infectious Disease Modelling and Analysis, Yale University, New Haven, CT, USA**
[4]**Faculty of Medicine, University of Toronto, Toronto, Ontario, M5S 1A8 Canada**

1 THE MODEL

We modelled the transmission of SARS–CoV-2 by extending an age-structured SEIR (Susceptible, Exposed, Infectious, Recovered) to include additional compartments of asymptomatic, pre-symptomatic, symptomatic, and isolation of infected individuals (Figure 1). We further included compartments to describe vaccination dynamics. The total population was divided into five age groups as specified in the main text. We omitted the demographic variables of births and deaths. With the variables described in Table 1, the model is expressed by the following system of equations:

$$
\begin{aligned}
S_a' &= -S_a\mathscr{I}_a - \xi_a S_a \\
V_a' &= \xi_a S_a - (1-\varepsilon_a)V_a\mathscr{I}_a \\
E_a' &= (1-q_a)S_a\mathscr{I}_a - \sigma E_a \\
\mathscr{E}_a' &= (1-q_a)(1-\varepsilon_a)V_a\mathscr{I}_a - \sigma\mathscr{E}_a \\
F_a' &= q_a S_a\mathscr{I}_a - \sigma F_a \\
\mathscr{F}_a &= q_a(1-\varepsilon_a)V_a\mathscr{I}_a - \sigma\mathscr{F}_a \\
A_a' &= p_a\sigma E_a + \rho_a\sigma\mathscr{E}_a - (1-g_a)\eta A_a - g_a\delta A_a \\
P_a' &= (1-p_a)\sigma E_a + (1-\rho_a)\sigma\mathscr{E}_a - (1-g_a)\theta P_a - g_a\delta P_a \\
I_a' &= (1-g_a)\theta P_a - (1-f_a)\gamma I_a - f_a\tau I_a \\
G_a' &= p_a\sigma F_a + \rho_a\sigma\mathscr{F}_a - \eta G_a \\
H_a' &= (1-p_a)\sigma F_a + (1-\rho_a)\sigma\mathscr{F}_a - \left(\frac{\gamma\theta}{\gamma+\theta}\right)H_a \\
B_a' &= g_a\delta A_a - \left(\frac{\delta\eta}{\delta-\eta}\right)B_a \\
C_a' &= g_a\delta P_a - \left(\frac{\delta\theta\gamma}{\delta\theta+\gamma(\delta-\theta)}\right)C_a \\
Q_a' &= f_a\tau I_a - \left(\frac{\tau\gamma}{\tau-\gamma}\right)Q_a
\end{aligned}
$$

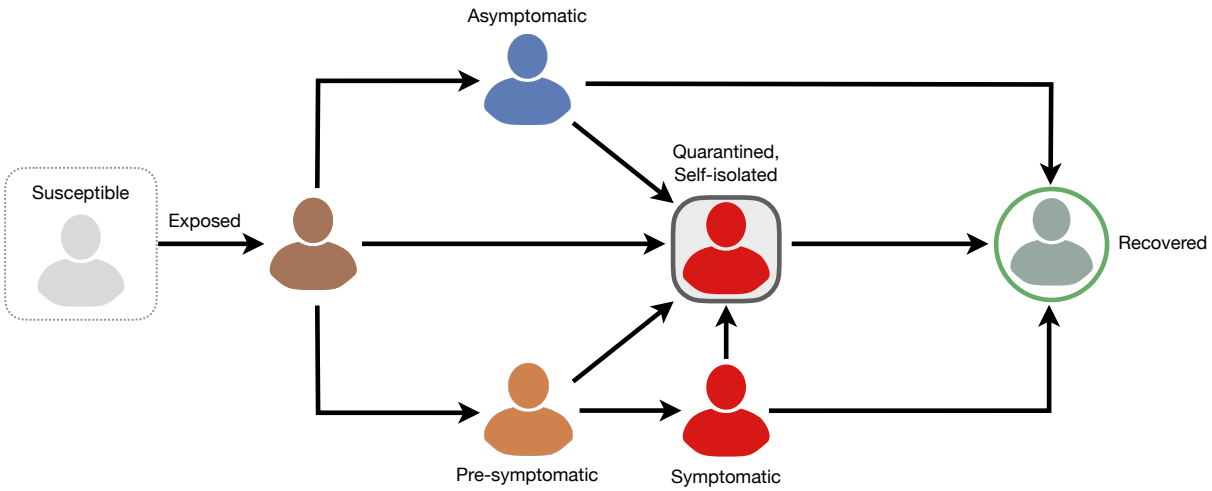

Figure 1. Schematic model diagram for disease transmission dynamics.

$$R_a' = (1-g_a)\eta A_a + (1-f_a)\gamma I_a + \eta G_a + \left(\frac{\gamma\theta}{\gamma+\theta}\right) H_a + \left(\frac{\delta\eta}{\delta-\eta}\right) B_a + \left(\frac{\delta\theta\gamma}{\delta\theta+\gamma(\delta-\theta)}\right) C_a + \left(\frac{\tau\gamma}{\tau-\gamma}\right) Q_a$$

with the force of infection $\mathscr{I}_a$, given by

$$\mathscr{I}_a = \beta\left(\sum_{j=1}^{6} M_{a,j}\frac{(P_j+\alpha A_j+I_j)}{N_j} + \sum_{j=1}^{6}\tilde{M}_{a,j}\frac{(C_j+\alpha B_j+Q_j+\alpha G_j+H_j)}{N_j}\right)$$

.

In this model, β is the transmission parameter (calibrated to the effective reproduction number $R_0 = 1.5$). The basic reproduction number R_0 denotes the average number of secondary infections by an infected individual before recovering and becoming immune (or dying) and measures the potential spread in the absence of containment interventions. We calibrated the transmission parameter by calculating the spectral radius of the next-generation matrix [1]. A full description of all model parameters are given in Table 2. Transmission between and within age groups was based on heterogeneous mixing with rates determined by age-specific contact matrices [2, 3] for regular contacts M and during isolation $\tilde{M}$:

$$M = \begin{array}{c} \begin{matrix} 0-4 & 5-10 & 11-18 & 19-49 & 50-64 & 65+ & \textbf{Age} \end{matrix} \\ \begin{bmatrix} 2.34 & 2.35 & 1.88 & 4.31 & 1.14 & 0.55 & 0-4 \\ 0.41 & 0.41 & 8.83 & 4.26 & 0.88 & 0.43 & 5-10 \\ 0.46 & 0.46 & 10.02 & 4.83 & 0.99 & 0.49 & 11-18 \\ 0.51 & 0.52 & 2.01 & 8.63 & 1.96 & 0.68 & 19-49 \\ 0.27 & 0.27 & 1.23 & 5.48 & 3.07 & 1.21 & 50-64 \\ 0.16 & 0.17 & 0.87 & 3.26 & 1.75 & 1.96 & 65+ \end{bmatrix} \end{array},$$

Table 1. Description of the model state variables.

Variable	Description
S_a	Susceptible in age group a
V_a	Vaccinated in age group a
E_a	Exposed in age group a (without vaccination)
$\mathscr{E}_a$	Exposed in age group a (with vaccination)
F_a	identified within latent period in age group a (without vaccination)
$\mathscr{F}_a$	identified within latent period in age group a (with vaccination)
A_a	Asymptomatic in age group a
P_a	Pre-symptomatic in age group a
I_a	Symptomatic in age group a
G_a	Asymptomatic isolated in age group a directly from latency
H_a	Pre-symptomatic isolated in age group a directly from latency
B_a	Asymptomatic isolated in age group a
C_a	Pre-symptomatic isolated in age group a
Q_a	Symptomatic isolated in age group a
R_a	Recovered in age group a
N_a	Population size of age group a

and

$$\tilde{M} = \begin{array}{c} \begin{matrix} 0-4 & 5-10 & 11-18 & 19-49 & 50-64 & 65+ & \textbf{Age} \end{matrix} \\ \begin{bmatrix} 0.64 & 0.65 & 0.53 & 1.21 & 0.32 & 0.15 \\ 0.11 & 0.12 & 2.3 & 1.21 & 0.25 & 0.12 \\ 0.12 & 0.13 & 2.8 & 1.35 & 0.28 & 0.14 \\ 0.14 & 0.15 & 0.56 & 2.41 & 0.55 & 0.19 \\ 0.07 & 0.08 & 0.34 & 1.53 & 0.86 & 0.34 \\ 0.05 & 0.05 & 0.24 & 0.91 & 0.49 & 0.55 \end{bmatrix} \begin{matrix} 0-4 \\ 5-10 \\ 11-18 \\ 19-49 \\ 50-64 \\ 65+ \end{matrix} \end{array}$$

where, in each matrix, the elements $\{m_{ij} \mid i, j \in (1, \cdots, 6)\}$ denote the average contact rates between age groups i and j.

In our model, all newly infected individuals start in the latent stage for an average period of $1/\sigma$ days. After this period has elapsed, infected individuals move to a communicable silent infection stage (i.e. asymptomatic or pre-symptomatic). Unlike asymptomatic cases, those who enter pre-symptomatic stage will develop symptoms. We assumed that all symptomatic cases initiate self-isolation within 24 hours of their symptom onset. The average infections periods in different stages of the disease are summarized in Table 2. Recovery from infection was assumed to provide immunity against re-infection during the simulations.

To include vaccination dynamics, we considered age-dependent vaccination rates to achieve a 40% vaccine coverage in adults within 1 year, with a distribution of 80% for age groups 50+ and 22% for individuals aged 19-49. Vaccination was assumed to prevent infection with an efficacy that is 50% lower than its efficacy against symptomatic disease (and 95% in

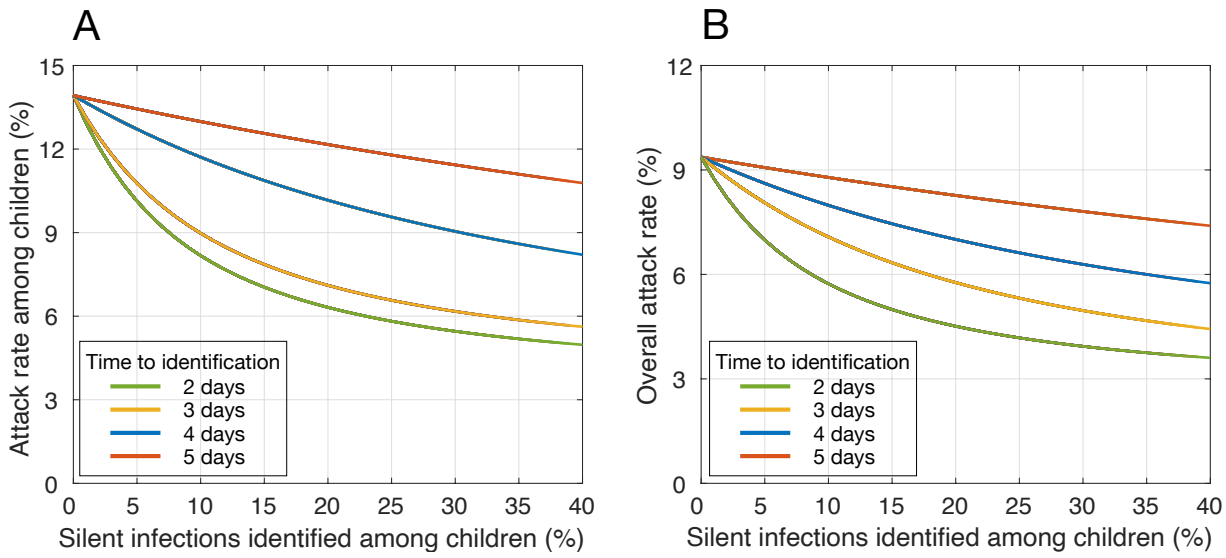

Figure 2. Reduction of attack rate achieved with different rates of silent infections (i.e., asymptomatic and pre-symptomatic) identified and isolated among children, when only adults were vaccinated. Colour curves indicate the average time from infection to identification. Susceptibility of children under 10 years old was reduced by 50% compared to other age groups. Vaccine efficacy was assumed to be 95% against symptomatic disease, but 50% lower against infection. Vaccination coverage of adults reached 40% within 1 year.

additional scenarios presented in Section 3 below). If infection occurred post-vaccination, we assumed the probability of developing symptomatic disease is reduced by a factor ρ_a (Table 2) corresponding to the vaccine efficacy of 95% [13].

For simulating the model, we used a non-standard numerical method to discretize the system and ran the simulations (in Matlab©) with introducing one latent individual into each age group in the model. The time horizon of simulations was 1 years.

2 RESULTS WITH REDUCED SUSCEPTIBILITY OF CHILDREN

Evidence is accumulating that young children may have a reduced susceptibility to SARS-CoV-2, with stronger immune responses that may prevent the development of symptomatic or severe disease [14, 15]. We therefore simulated the model by considering a 50% reduction of susceptibility for children under 10 years of age. Qualitatively, the effect of identifying silent infections on the reduction of attack rates remains intact and the speed of identification is critical for outbreak control. Projected attack rates for the range of 2-5 days delay in identification of silent infections among children, when only adults are vaccinated, are presented in Figure 2.

3 RESULTS WITH 95% VACCINE EFFICACY AGAINST INFECTION

In the absence of data on vaccine efficacy against infection, we further simulated the model with the same efficacy of 95% against symptomatic disease, while also considering 50% reduced susceptibility for children under 10 years old. The results presented in Figure 3 below illustrate a qualitative similar patterns to those presented in Figure 2 of the main text, indicating that the sharpest decline of attack rates occur with rapid identification of $0-15\%$ silent infections among children within 2-3 days post-infection.

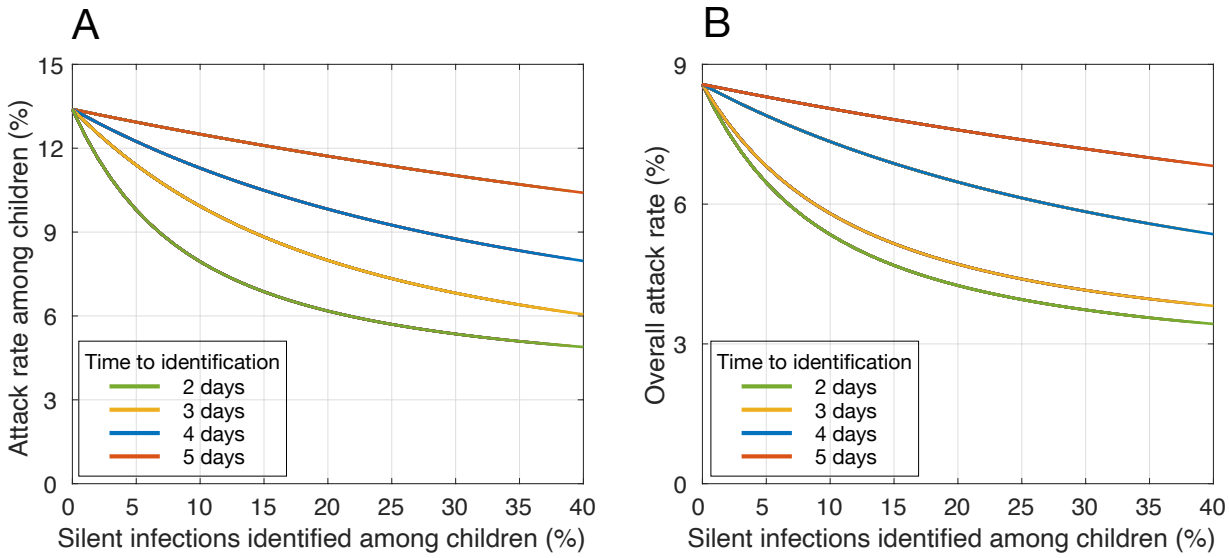

Figure 3. Reduction of attack rate achieved with different rates of silent infections (i.e., asymptomatic and pre-symptomatic) identified and isolated among children, when only adults were vaccinated. Colour curves indicate the average time from infection to identification. Susceptibility of children under 10 years old was reduced by 50% compared to other age groups. Vaccine efficacy was assumed to be 95% against both infection and symptomatic disease. Vaccination coverage of adults reached 40% within 1 year.

Table 2. Description of the model parameters and their associated values.

Parameter	Description	Value	Source
β	Transmission parameter calibrated to $R_0 = 1.5$	0.0238, 0.0241	[4]
α	Relative transmission of asymptomatic	0.26	[5]
$1/\sigma$	Average latent period	2.2 days	Calculated by subtracting $1/\theta$ from the average 5.2 days of incubation period [6]
q_a	% of infected individuals identified during latent period	$0-1$	Varied
p_a	% of infected individuals that are asymptomatic		
	▷ Age group: $0-4$	30%	[7]
	▷ Age group: $5-10$	30%	
	▷ Age group: $11-18$	37.3%	
	▷ Age group: $19-49$	32.8%	
	▷ Age group: $50-64$	32.8%	
	▷ Age group: $65+$	18.8%	
g_a	% of infected individuals identified during asymptomatic and pre-symptomatic stages	$0-100\%$	Varied
$1/\eta$	Average infectious period of asymptomatic infection	5 days	[8, 9]
$1/\delta$	Time to identification of silent infections during asymptomatic and pre-symptomatic stages	$0.8-2.8$ days	Assumed
$1/\theta$	Average duration of pre-symptomatic stage	3 days	[8, 10]
f_a	% of symptomatic cases who self-isolate	100%	Assumed
$1/\gamma$	Average infectious period post-symptom onset	3.2 days	[8, 9]
$1/\tau$	Average time to self-isolation post-symptom onset	24 hours	Assumed
ε	Baseline vaccine efficacy in preventing infection	95%	[11, 12]
ρ_a	% of vaccinated individuals who develop asymptomatic infection if infected post-vaccination	$p_a \leq \rho_a \leq 100\%$	Calculated by $\rho_a = 1-(1-p_a)(1-\varepsilon)$
ξ_a	vaccination rate, Calculated to achieve the annual coverage		
	▷ Age groups: $0-18$ (0% coverage)	0	
	▷ Age group: $19-49$ (22% coverage)	7.935×10^{-4}/day	
	▷ Age groups: $50-64$ (80% coverage)	5.649×10^{-3}/day	
	▷ Age groups: $65+$ (80% coverage)	5.233×10^{-3}/day	

REFERENCES

[1] Diekmann, Odo et al. “On the definition and the computation of the basic reproduction ratio R 0 in models for infectious diseases in heterogeneous populations”. In: *Journal of mathematical biology* 28.4 (1990), pp. 365–382.

[2] Mossong, Joël et al. “Social Contacts and Mixing Patterns Relevant to the Spread of Infectious Diseases”. In: *PLoS Medicine* 5.3 (Mar. 25, 2008). Ed. by Steven Riley, e74. ISSN: 1549-1676. DOI: 10.1371/journal.pmed.0050074. (Visited on 05/22/2020).

[3] Jarvis, Christopher I. et al. “Quantifying the impact of physical distance measures on the transmission of COVID-19 in the UK”. In: *BMC Medicine* 18.1 (Dec. 2020), p. 124. ISSN: 1741-7015. DOI: 10.1186/s12916-020-01597-8. (Visited on 11/17/2020).

[4] *Rt COVID-19*. URL: https://rt.live/ (visited on 11/17/2020).

[5] Sayampanathan, Andrew A et al. “Infectivity of asymptomatic versus symptomatic COVID-19”. In: *Lancet* 20.S0140-6736 (2020), pp. 32651–32659.

[6] Li, Qun et al. “Early Transmission Dynamics in Wuhan, China, of Novel Coronavirus-Infected Pneumonia”. In: *The New England Journal of Medicine* 382.13 (2020), pp. 1199–1207. ISSN: 1533-4406. DOI: 10.1056/NEJMoa2001316.

[7] Buitrago-Garcia, Diana et al. “Occurrence and transmission potential of asymptomatic and presymptomatic SARS-CoV-2 infections: A living systematic review and meta-analysis”. In: *PLOS Medicine* 17.9 (Sept. 22, 2020). Ed. by Nathan Ford, e1003346. ISSN: 1549-1676. DOI: 10.1371/journal.pmed.1003346. (Visited on 11/17/2020).

[8] Moghadas, Seyed M. et al. “The implications of silent transmission for the control of COVID-19 outbreaks”. In: *Proceedings of the National Academy of Sciences* (July 6, 2020), p. 202008373. ISSN: 0027-8424, 1091-6490. DOI: 10.1073/pnas.2008373117. (Visited on 07/28/2020).

[9] Li, Ruiyun et al. “Substantial undocumented infection facilitates the rapid dissemination of novel coronavirus (SARS-CoV-2)”. In: *Science* 368.6490 (May 1, 2020). ISSN: 0036-8075, 1095-9203. DOI: 10.1126/science.abb3221. (Visited on 11/17/2020).

[10] He, Xi et al. “Temporal dynamics in viral shedding and transmissibility of COVID-19”. In: *Nature Medicine* (Apr. 15, 2020). ISSN: 1546-170X. DOI: 10.1038/s41591-020-0869-5. (Visited on 04/16/2020).

[11] Moderna. *Moderna’s COVID-19 Vaccine Candidate Meets its Primary Efficacy Endpoint in the First Interim Analysis of the Phase 3 COVE Study — Moderna, Inc.* en. Tech. rep. Nov. 2020. URL: https://investors.modernatx.com/news-releases/news-release-details/modernas-covid-19-vaccine-candidate-meets-its-primary-efficacy/ (visited on 11/17/2020).

[12] Pfizer and BioNTech. *Pfizer and BioNTech Announce Vaccine Candidate Against COVID-19 Achieved Success in First Interim Analysis from Phase 3 Study — Pfizer*. Tech. rep. URL: https://www.pfizer.com/news/press-release/press-release-detail/pfizer-and-biontech-announce-vaccine-candidate-against (visited on 11/17/2020).

[13] Polack, Fernando P et al. "Safety and efficacy of the BNT162b2 mRNA covid-19 vaccine". In: *New England Journal of Medicine* (2020).

[14] Tosif, Shidan et al. "Immune responses to SARS-CoV-2 in three children of parents with symptomatic COVID-19". In: *Nature communications* 11.1 (2020), pp. 1–8.

[15] Steinman, Jonathan Baruch et al. "Reduced development of COVID-19 in children reveals molecular checkpoints gating pathogenesis illuminating potential therapeutics". In: *Proceedings of the National Academy of Sciences* 117.40 (2020), pp. 24620–24626.